Phys Chem Minerals (2005) 32: 13–18
DOI 10.1007/s00269-004-0432-9

ORIGINAL PAPERS

Catherine Leyx · J. Cornelis Van Miltenburg
Christian Chopin · Lado Cemič

Heat-capacity measurements and absolute entropy of ε-Mg_2PO_4OH

Received: 29 July 2004 / Accepted: 13 October 2004 / Published online: 8 February 2005

Abstract The low-temperature heat capacity of ε-Mg_2PO_4OH was measured between 10 and 400 K by adiabatic calorimetry. No phase transition was observed over this temperature range. A relative enthalpy increment of 22,119 J mol^{-1} and an absolute entropy value of 127.13 ± 0.25 J mol^{-1} K^{-1} at 298.15 K are derived from the results. The low-temperature heat-capacity data are compared with the DSC data obtained from 143 K to 775 K and show marginal differences in the common temperature range. The latter data are fitted by the polynomial

$$C_p = \{316.62 - 2957\,T^{-0.5} - 563350\,T^{-2} + 955.55 \times 10^5\,T^{-3}\}\,\mathrm{J\,K^{-1}\,mol^{-1}},$$

which allows extrapolation to high temperatures.

Keywords Adiabatic calorimetry · DSC calorimetry · Magnesium phosphate · Heat capacity · Entropy

Introduction

Magnesium phosphates have received surprisingly little attention from a thermodynamic point of view. They are yet of industrial interest, for instance as bonding materials in refractories and mortars (Lyon et al. 1966), as rapid-setting cements (Sarkar 1990; Yang et al. 2000) or as fertiliser (e.g. Bolland et al. 1992; Sata 1997); they are also of medical interest in urinary stones (Sutor 1974) and in biomaterials (Driessens et al. 1995). As rock-forming minerals, although less common than other phosphates like apatite, Mg-phosphates play an important role in late-stage metasomatic processes around alkaline intrusive rocks (as shown by the spectacular veins of bobierrite, $Mg_3(PO_4)_2{\cdot}8H_2O$, and kovdorskite, $Mg_2PO_4OH{\cdot}3H_2O$, in the Kola peninsula); they are also potential petrological indicators in metamorphic rocks owing to their numerous polymorphic relations. Indeed, early synthesis work has revealed five polymorphs of Mg_2PO_4OH (labelled α to ε, Raade 1990) and three polymorphs of $Mg_3(PO_4)_2$ (e.g. Berthet et al. 1972; Annersten and Nord 1980; Théodoret et al. 1987; Jaulmes et al. 1997). Experimental phase-equilibrium studies (Brunet and Vielzeuf 1996; Brunet et al. 1998; Leyx et al. 2002) have explored the relations of the $Mg_3(PO_4)_2$ polymorphs with four of the Mg_2PO_4OH polymorphs and the mineral phosphoellenbergerite, ideally $Mg_{14}(PO_4)_6(PO_3OH)_2(OH)_6$. The $Mg_3(PO_4)_2$ polymorphs include a low-pressure polymorph, the mineral farringtonite found in meteorites, and a high-pressure one, the Mg analogue of the pegmatite mineral sarcopside. Among the polymorphs of Mg_2PO_4OH, althausite (δ) and holtedahlite (γ) were shown to be intermediate-pressure minerals, ε to be the low-pressure and high-temperature phases, and β, which is the hydroxyl analogue of wagnerite Mg_2PO_4F, to be the high-pressure form. The latter phase and phosphoellenbergerite turned out to be high-pressure minerals actually encountered in ultrahigh-pressure metamorphic rocks (Brunet et al. 1998). However, this large body of phase-equilibrium data remained so far unamenable to thermodynamic treatment because of the dearth of thermodynamic data even in a simple system as $MgO–P_2O_5–H_2O$. Indeed, farringtonite being the sole phase for which enthalpy of formation, heat capacity, and entropy were known (Stevens and Turkdogan 1954; Oetting and McDonald 1963;

Software information: WINDOWS operating system, WORD word processing, SigmaPlot diagrams exported in tiff format.

C. Leyx · C. Chopin (✉)
Laboratoire de Géologie, UMR 8538 du CNRS, Ecole normale supérieure, 24 rue Lhomond, 75005 Paris, France
E-mail: chopin@geologie.ens.fr
Tel.: +33-1-44322279
Fax: +33-1-44322000

J. C. Van Miltenburg
Chemical Thermodynamics Group, State University of Utrecht, Padualaan 8, Utrecht, 3508 TB, The Netherlands

L. Cemič
Institut für Geowissenschaften der Christian-Albrechts-Universität Kiel, Olshausenstrasse 40, Kiel, 24098, Germany

both reexamined by Lodders 1999), it is necessary to have one more "anchor phase" in this system to extract the thermodynamic properties (entropy, enthalpy of formation) of phosphoellenbergerite and the Mg_2PO_4OH polymorphs from the phase-equilibrium data. The low-pressure phase ε-Mg_2PO_4OH was therefore an obvious target for calorimetric work as it could be more easily synthesised in large enough batches. We report here, low-temperature adiabatic heat-capacity measurements as well as intermediate- to high-temperature differential scanning calorimetry (DSC) results on this polymorph. The accurate entropy value derived will set tight constraints on the enthalpy of formation through the high correlation existing between entropy and enthalpy values extracted from phase equilibrium data.

Experimental techniques

Sample preparation and characterization

The ε-Mg_2PO_4OH polymorph was synthesised hydrothermally at 60 MPa and 620 K in externally heated Tuttle-type cold-seal pressure vessels for an approximate duration of 2 months (see Brunet et al. 1998 for experimental details). It was prepared from a stoichiometric mixture of MgO (Alfa Aesar, 99.95%, fired at 1,300°C before mixing) added to $NH_4H_2PO_4$ (Aldrich, 99.999%), reacted with water, and baked at 600°C for 2 h. The mixture was enclosed with 10 wt% deionised water in gold capsules of 3 mm or 4 mm outer diameter, which were sealed by arc welding. Nine runs were required to synthesise 5.6 g of the compound, each of them yielding 500–800 mg of ε-Mg_2PO_4OH, with a grain size in the range 1–10 μm. Each batch was sampled in several places along the length of the capsule, analysed by X-ray powder diffraction and checked for purity. The cell parameters obtained by whole-pattern refinement are $a = 8.2416$ (3), $b = 6.1338$ (2), $c = 7.4120$ (3) Å, $V = 374.69$ (3) Å^3, in good agreement with Raade and Rømming (1986) and Raade (1990) data. No extra phase was detected in this way, nor by examination under the scanning electron microscope.

Adiabatic calorimetry

Measurements were performed in the CAL V calorimeter of the Chemical Thermodynamics Group, Utrecht (Van Miltenburg et al. 1987, 1998). This adiabatic calorimeter consists of a cryostat for liquid helium and liquid nitrogen and a measuring compartment located below the liquid-helium holder. The measuring part consists of a sample vessel (volume 11 cm^3) surrounded by two temperature-controlled shields. The inner shield is controlled to the same temperature as the vessel, the outer shield to about 10 K below the temperature of the inner shield. A regulated heater for the wires is used to bring the wire bundle going to the vessel to the same temperature as the vessel. In the insert of the vessel a 30Ω Rh/Fe resistance calibrated by Oxford Instruments is used as thermometer, and a 100-Ω-resistance wire is wound bifilarly around the insert and serves as the heater. The calibration of the thermometer is based on the ITS-90 temperature scale (Preston-Thomas 1990). The accuracy of the heat-capacity measurements was checked by measuring *n*-heptane and synthetic sapphire. No deviations from the recommended values larger than 0.2% were found.

Before the compound was loaded in the calorimeter vessel, it was evacuated at about 100°C for several hours and stored under vacuum for 5 days in order to remove physically attached water. A mass of 5.6 g was loaded in the vessel, which was evacuated and then filled with about 1,000 Pa of helium before closing. The helium gas served as a heat-exchange gas. Measurements were made in the intermittent mode, using stabilization periods of about 600 s and heat input periods of about 500 s. Below 30 K, shorter time periods were used. Several measurement series were made, covering each temperature region at least twice.

Differential scanning calorimetry

The higher-temperature measurements were performed with a Perkin Elmer DSC 7 differential scanning calorimeter at Institut für Geowissenschaften, Kiel University. The experimental technique was similar to that of Bosenick et al. (1996), Fasshauer et al. (1998) and Benisek et al. (1999). In the low-temperature region (143–323 K), the measurements were made under a flow of helium gas while the calorimeter block was kept at 93 ± 5 K with liquid nitrogen, whereas, in the high-temperature region (323–775 K), a flow of dried nitrogen was used, with the calorimeter block thermostated at 293 ± 1 K. Known melting points and phase transitions were used for temperature calibration (the phase transition and the melting of cyclohexane at 186.09 K and 279.69 K, respectively, the melting of In at 429.75 K and the phase transition of Li_2SO_4 at 851.0 K); temperature accuracy is assumed to be ± 1 K as determined by Bosenick et al. (1996). A single-crystal synthetic corundum was used as the C_p-calibration standard; its heat capacity was taken from Ditmars and Douglas (1971).

The standard and the sample (around 60 mg) were placed into Au pans. The measurements were performed using the step-scanning method described in Bosenick et al. (1996), with a heating rate of 20 K min^{-1} over temperature intervals of 100 K.

Results

Adiabatic calorimetry

The experimental data given in Table 1 form a continuously measured set from 10 K to 400 K. As the other data series did not show deviations above the

Table 1 Experimental molar heat capacities of ε-Mg_2PO_4OH (adiabatic calorimetry)

T (K)	C_p (J K^{-1} mol^{-1})	T (K)	C_p (J K^{-1} mol^{-1})	T (K)	C_p (J K^{-1} mol^{-1})	T (K)	C_p (J K^{-1} mol^{-1})	T (K)	C_p (J K^{-1} mol^{-1})
7.17	0.20	84.16	36.30	158.61	85.82	227.62	119.42	296.15	144.01
8.98	0.21	85.03	36.90	160.55	86.93	229.25	120.12	299.11	144.82
11.09	0.24	86.66	38.09	162.49	88.04	230.89	120.80	302.07	145.58
13.13	0.25	88.24	39.20	164.41	89.04	232.51	121.44	305.02	146.57
15.28	0.45	89.09	39.81	166.32	90.16	234.13	122.12	307.97	147.57
17.47	0.53	91.33	41.38	168.22	91.20	235.75	122.73	310.92	148.43
19.67	0.76	91.45	41.49	170.11	92.25	237.37	123.47	313.88	149.29
21.97	1.12	93.74	43.13	171.98	93.26	238.97	124.05	316.84	150.05
24.40	1.64	94.31	43.48	173.84	94.21	240.58	124.67	319.79	150.96
26.92	2.30	95.98	44.70	175.70	95.23	242.18	125.31	322.74	151.86
29.59	3.05	97.20	45.52	177.54	96.21	243.77	125.93	325.70	152.62
32.41	4.10	98.17	46.26	179.37	97.16	245.36	126.57	328.65	153.68
35.28	5.34	100.01	47.53	181.20	98.10	246.95	127.18	331.60	154.44
38.19	6.52	100.31	47.76	183.01	99.03	248.53	127.82	334.55	155.26
40.65	7.77	102.75	49.59	184.82	99.92	250.11	128.48	337.50	156.04
42.94	9.01	105.41	51.45	186.62	100.83	251.69	129.16	340.46	156.78
45.28	10.28	108.02	53.50	188.40	101.75	253.26	129.65	343.40	157.44
47.67	11.70	110.57	55.19	190.18	102.62	254.83	129.87	346.36	158.15
50.10	13.15	113.07	56.88	191.96	103.49	256.40	130.66	349.31	158.89
52.57	14.65	115.52	58.52	193.72	104.30	257.97	131.26	352.25	159.61
55.07	16.25	117.94	60.11	195.48	105.16	259.53	131.91	355.21	160.42
57.61	17.88	120.32	61.12	197.23	106.05	261.08	132.60	358.16	161.12
57.91	18.07	122.66	63.22	198.97	106.87	262.63	133.16	361.11	161.66
60.18	19.58	124.97	64.87	200.70	107.61	264.18	133.79	364.06	162.40
61.15	20.23	127.24	66.44	202.43	108.45	265.73	134.10	367.02	163.14
62.78	21.34	129.49	67.89	204.15	109.28	267.27	134.50	369.97	163.78
64.46	22.39	131.71	69.39	205.86	110.01	268.81	134.99	372.92	164.41
65.41	23.11	133.91	70.78	207.57	110.83	270.35	135.54	375.87	165.27
67.82	24.73	136.08	72.15	209.27	111.58	271.88	136.12	378.82	165.89
68.06	24.93	138.23	73.54	210.97	112.37	273.42	136.38	381.78	166.46
70.74	26.79	140.36	74.84	212.66	113.06	274.94	136.84	384.73	167.07
71.23	27.25	142.46	76.16	214.34	113.85	276.47	137.37	387.68	167.70
73.43	28.68	144.54	77.45	216.02	114.53	277.99	137.92	390.63	168.34
74.68	29.17	146.60	78.69	217.69	115.26	279.51	138.35	393.58	168.82
76.14	30.57	148.64	79.95	219.36	116.04	281.03	138.89	396.53	169.51
78.18	32.01	150.67	81.19	221.02	116.71	282.55	139.32	399.49	169.88
78.86	32.51	152.67	82.34	222.68	117.38	288.46	140.94		
81.56	34.42	154.67	83.54	224.33	118.12	290.23	141.91		
81.67	34.45	156.64	84.66	225.98	118.81	293.19	142.91		

reproducibility of the apparatus (about 1% below 30 K, 0.05–0.1% between 30 K and 100 K, and 0.03% above 100 K), they are not included in Table 1. In Fig. 1 however, all experimental data are given. No indication of a phase transition was found in this temperature range [implying that the ε phase remained metastable with respect to the low-temperature α phase (Raade 1990)] and the data were interpolated for every degree. The results are presented in steps of 5 K or 10 K in Table 2.

Calculation of the absolute entropy S_0 and of the relative enthalpy increment ($H(T)$–$H(0)$)

From the low-temperature heat-capacity data set, the entropy and enthalpy values, given at selected temperatures in Table 2, were calculated by numerical integration. For this calculation, starting values of the entropy and enthalpy are needed. The heat capacity of the compound dropped rapidly below 10 K and the difference with the empty-vessel experiment became too small to give reliable results. The extrapolation of the heat capacity to 0 K was made by assuming that below 10 K, the Debye low-temperature relation, $C_p = \alpha\ T^3$, could be used. The value found for α by fitting the raw data between 13 K and 25 K is 0.000109 J K^{-4} mol^{-1}, resulting in the starting values of 0.036 J K^{-1} mol^{-1} for the entropy at 10 K and 0.272 J mol^{-1} for $H(10)-H(0)$. Integration of the $C_p(T)/T$ function between 0 K and 298.15 K yielded a standard entropy value of 127.13 J mol^{-1} K^{-1}, for which an uncertainty of 0.25 J mol^{-1} K^{-1} is proposed, on the basis of the accuracy of the C_p measurement.

High-temperature heat capacity

The mean of the C_p values obtained from six series of DSC measurements between 143 K and 775 K are given in Table 3 together with the standard deviation. Figure 2 compares the data series obtained by adiabatic and

Table 2 Thermodynamic properties at selected temperatures for ε-Mg_2PO_4OH

T (K)	$C^{\circ}_{p,\,m}$ (J K^{-1} mol^{-1})	S°_{m} (J K^{-1} mol^{-1})	ΔH°_{m} (J mol^{-1})
10	0.11	0.04	0.27
20	0.81	0.27	4.04
25	1.79	0.55	10.4
30	3.18	1.00	22.9
35	5.22	1.65	44.0
40	7.43	2.44	73.6
45	10.13	3.47	117
50	13.10	4.69	176
55	16.20	6.08	249
60	19.46	7.63	338
65	22.80	9.32	444
70	26.27	11.15	567
75	29.44	13.07	706
80	33.33	15.12	865
85	36.88	17.21	1,038
90	40.45	19.43	1,232
95	43.98	21.70	1,442
100	47.53	24.04	1,670
105	51.16	26.44	1,917
110	54.81	28.91	2,182
115	58.17	31.42	2,464
120	60.93	33.96	2,763
130	68.24	39.14	3,410
140	74.62	44.43	4,125
150	80.78	49.79	4,902
160	86.61	55.19	5,739
170	92.19	60.61	6,633
180	97.48	66.03	7,581
190	102.53	71.44	8,582
200	107.30	76.82	9,631
210	111.92	82.17	10,727
220	116.30	87.47	11,868
230	120.43	92.73	13,052
240	124.44	97.94	14,276
250	128.43	103.10	15,541
260	132.12	108.21	16,843
270	135.41	113.26	18,181
280	138.52	118.24	19,551
290	141.81	123.16	20,951
298.15	**144.57**	**127.13**	**22,119**
300	145.04	128.02	22,387
310	148.16	132.83	23,853
320	151.03	137.58	25,348
330	154.03	142.27	26,874
340	156.67	146.91	28,427
350	159.06	151.48	30,006
360	161.44	156.00	31,609
370	163.79	160.46	33,235
380	166.11	164.86	34,885

Molar mass = 160.5887 g mol^{-1}

DSC calorimetry, which overlap in the range 143–400 K. Over this range, the DSC data are marginally but consistently lower than the 'low-temperature' adiabatic data. Both data series are closest near 220 K with a minimum difference of 0.6%; the discrepancy worsens toward lower temperatures to reach 3.8% at 143 K and remains near 1.7% up to the highest temperature (400 K). However, the low-temperature adiabatic data set remains within one standard deviation of the less precise DSC data over the whole range.

For practical purposes, in particular the handling of high-temperature phase-equilibrium data, the data set

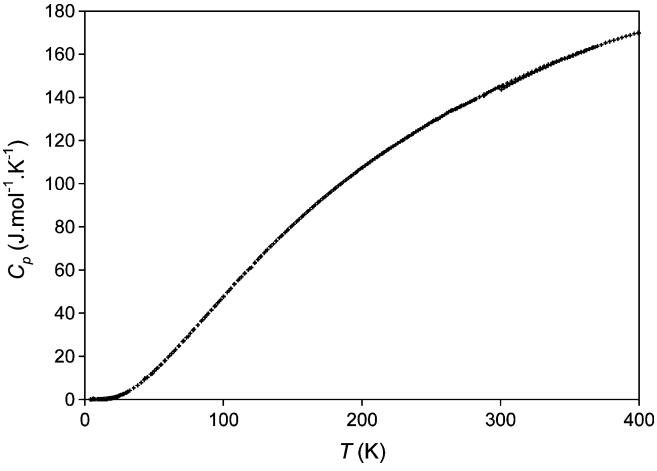

Fig. 1 Experimental heat-capacity data of ε-Mg_2PO_4OH (adiabatic calorimetry)

obtained at high temperature was fitted with the polynomial representation proposed by Berman and Brown (1985),

$$C_p = k_0 + k_1 T^{-0.5} + k_2 T^{-2} + k_3 T^{-3} \text{ (where } k_1 \text{ and } k_2 \leq 0).$$

This formulation ensures that extrapolation outside the range of measurement satisfies the high-temperature Dulong and Petit limit. The parameters obtained from the fit of the whole DSC data set are reported in Table 3; the resulting curve is shown as the solid line in Fig. 2.

Discussion and perspective

The results obtained here are a first step toward the derivation of an internally consistent set of thermodynamic properties for the MgO–P_2O_5–H_2O system. As the H_f and S_0 values derived from phase-equilibrium constraints for an 'unknown' phase are highly correlated, the precise knowledge of an entropy value as determined here sets in turn tight constraints on the H_f value that can be extracted from phase-equilibrium data, for instance from experimental brackets on a reaction like

$$2\,\varepsilon\text{-}Mg_2PO_4OH + Al_2O_3 \text{ corundum} = Mg_3(PO_4)_2 \text{ farringtonite} + MgAl_2O_4 \text{ spinel} + H_2O$$

(cf. Leyx et al. 2002), in which ε-Mg_2PO_4OH is the only unknown.

The entropy value derived here for ε-Mg_2PO_4OH may be compared with estimates made using summation methods, for instance the one proposed by Holland (1989), based on the volume-corrected additivity of fictive oxide components and extended to phosphates by Brunet et al. (2004). Using Holland's (1989) $S-$ values for $^{[6]}MgO$ and high-entropy H_2O (as the OH groups are essentially unbonded, Raade and Rømming 1986), Brunet et al. (2004) values for $^{[5]}MgO$ and P_2O_5, and an ε-Mg_2PO_4OH standard volume of 56.3 cm^3 mol^{-1}

Table 3 Experimental molar heat capacities of ε-Mg_2PO_4OH (differential scanning calorimetry)

T (K)	C_p (J K^{-1} mol^{-1})	σ (C_p) (%)	T (K)	C_p (J K^{-1} mol^{-1})	σ (C_p) (%)	T (K)	C_p (J K^{-1} mol^{-1})	σ (C_p) (%)
143.15	73.57	5.70	358.15	158.28	2.59	573.15	192.54	2.04
148.15	76.93	5.62	363.15	159.45	2.58	578.15	193.22	2.10
153.15	79.98	5.65	368.15	160.57	2.53	583.15	193.96	2.26
158.15	83.36	5.65	373.15	161.66	2.56	588.15	194.64	2.48
163.15	86.16	5.58	378.15	162.76	2.53	593.15	195.32	2.78
168.15	89.36	5.54	383.15	163.79	2.51	598.15	196.17	3.07
173.15	91.86	5.19	388.15	164.80	2.50	603.15	196.38	3.20
178.15	94.70	5.33	393.15	165.77	2.51	608.15	196.70	3.03
183.15	97.29	5.05	398.15	166.75	2.51	613.15	196.93	2.71
188.15	99.92	5.05	403.15	167.66	2.52	618.15	197.22	2.60
193.15	102.30	4.64	408.15	168.60	2.54	623.15	197.56	2.56
198.15	104.79	4.53	413.15	169.49	2.53			
203.15	107.13	4.05	418.15	170.39	2.61	643.15	198.51	1.98
208.15	109.72	3.99	423.15	171.32	2.60	648.15	198.96	2.02
213.15	111.92	3.25				653.15	199.45	2.01
218.15	114.30	3.04	443.15	174.05	2.58	658.15	199.92	1.97
223.15	116.90	2.81	448.15	174.86	2.54	663.15	200.37	2.00
			453.15	175.76	2.52	668.15	200.81	1.98
243.15	123.62	2.97	458.15	176.59	2.46	673.15	201.24	1.94
248.15	125.45	2.92	463.15	177.44	2.43	678.15	201.61	2.00
253.15	127.76	3.10	468.15	178.29	2.38	683.15	202.08	2.02
258.15	130.48	3.05	473.15	179.07	2.39	688.15	202.41	2.03
263.15	130.73	3.24	478.15	179.79	2.35	693.15	202.89	2.02
268.15	131.87	3.27	483.15	180.54	2.34	698.15	203.35	2.04
273.15	133.53	3.22	488.15	181.29	2.32	703.15	203.81	2.10
278.15	135.17	3.29	493.15	182.03	2.32	708.15	204.24	2.14
283.15	136.91	3.29	498.15	182.72	2.30	713.15	204.77	2.19
288.15	138.37	3.21	503.15	183.42	2.37	718.15	205.29	2.21
293.15	140.14	3.23	508.15	184.17	2.35	723.15	205.96	2.41
298.15	141.60	3.00	513.15	184.83	2.34			
303.15	143.34	3.15	518.15	185.51	2.38	743.15	206.63	2.12
308.15	144.90	2.76	523.15	185.88	2.40	748.15	207.03	1.98
313.15	146.46	2.74				753.15	207.53	1.96
318.15	148.03	2.40	543.15	188.27	2.15	758.15	208.03	1.99
323.15	149.72	2.37	548.15	188.92	2.15	763.15	208.49	2.00
			553.15	189.64	2.07	768.15	208.96	1.97
343.15	154.52	2.79	558.15	190.36	2.06	773.15	209.44	1.99
348.15	155.80	2.72	563.15	190.96	2.11			
353.15	157.06	2.67	568.15	191.77	2.00			

Berman and Brown (1985) fit: $C_p = 316.62 - 2957\ T^{-0.5} - 563350\ T^{-2} + 955.55\times10^5\ T^{-3}$

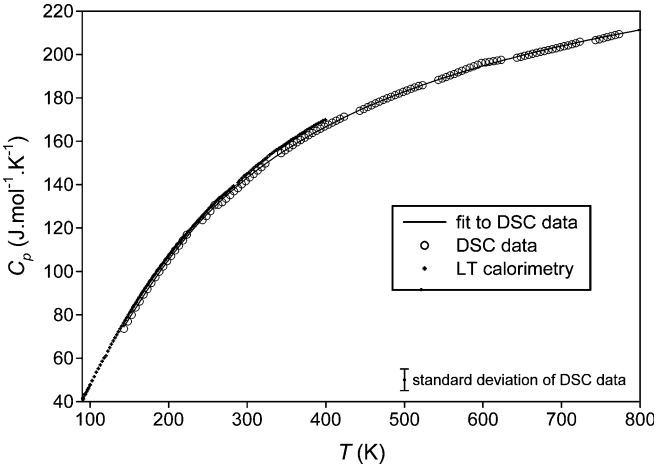

Fig. 2 Comparison between low-temperature and high-temperature heat-capacity data of ε-Mg_2PO_4OH

(Raade and Rømming 1986), we obtain an estimated standard entropy of 118.9(5.8) J mol^{-1} K^{-1} for ε-Mg_2PO_4OH, which is about 6% lower than, and therefore only marginally consistent with the calorimetric value. This discrepancy may be due to the narrow basis of thermodynamic data on which the $S-V$ parameters for $^{[5]}MgO$ and P_2O_5 were derived (Brunet et al. 2004); it emphasises the need for additional calorimetric measurements on a variety of phosphates.

Acknowledgements We thank Mrs Kluge, Kiel, for the DSC measurements, Fabrice Brunet and Peter Schmid-Beurmann for numerous discussions, Gunnar Raade and the anonymous referee for their careful reviews.

References

Annersten H, Nord AG (1980) A high pressure phase of magnesium orthophosphate. Acta Chem Scand 34:389–390

Benisek A, Dachs E, Cemič L (1999) Heat capacities of Tschermak substituted Fe-biotite. Contrib Mineral Petrol 135:53–61

Berman RG, Brown TH (1985) Heat capacity of minerals in the system Na_2O–K_2O–CaO–MgO–FeO–Fe_2O_3–Al_2O_3–SiO_2–TiO_2–H_2O–CO_2: representation, estimation, and high temperature extrapolation. Contrib Mineral Petrol 89:168–183

Berthet G, Joubert JC, Bertaut EF (1972) Vacancies ordering in new metastable orthophosphates $(Co_3)P_2O_8$ and $(Mg_3)P_2O_8$ with olivine-related structure. Z Kristallogr 136:98–105

Bolland MDA, Glencross RN, Gilkes RJ, Kumar V (1992) Agronomic effectiveness of partially acidulated rock phosphate and fused calcium-magnesium phosphate compared with superphosphate. Fertil Res 32:169–183

Bosenick A, Geiger CA, Cemič L (1996) Heat capacity measurements of synthetic pyrope-grossular garnets between 320 and 1000 K by differential scanning calorimetry. Geochim Cosmochim Acta 60:3215–3227

Brunet F, Vielzeuf D (1996) The farringtonite / $Mg_3(PO_4)_2$-II transformation: a new curve for pressure calibration in piston-cylinder apparatus. Eur J Mineral 8:349–354

Brunet F, Chopin C, Seifert F (1998) Phase relations in the MgO–P_2O_5–H_2O system and the stability of phosphoellenbergerite: petrological implications. Contrib Mineral Petrol 131:54–70

Brunet F, Morineau D, Schmid-Beurmann P (2004) Heat-capacity of lazulite, $MgAl_2(PO_4)_2(OH)_2$, from 35 to 298 K and a (S–V) value for P_2O_5 to estimate phosphates entropy. Mineral Mag 68:123–134

Ditmars DA, Douglas TB (1971) Measurements of the relative enthalpy of pure α-Al_2O_3 (NBS heat capacity and enthalpy reference material No. 720) from 273 to 1173 K. J Res 75A:401–420

Driessens FCN, Boltong MG, Zapatero MI, Verbeeck RMH, Bonfield W, Bermudez O, Fernandez E, Ginebra MP, Planell JA (1995) In-vivo behavior of 3 calcium-phosphate cements and a magnesium phosphate cement. J Mater Sci - Mater in Medicine 6:272–278

Fasshauer DW, Chatterjee ND, Cemič L (1998) A thermodynamic analysis of the system $LiAlSiO_4$-$NaAlSiO_4$-Al_2O_3-SiO_2-H_2O based on new heat capacity, thermal expansion, and compressibility data for selected phases. Contrib Mineral Petrol 133:186–198

Holland TJB (1989) Dependence of entropy on volume for silicate and oxide minerals: A review and a predictive model. Am Mineral 74:5–13

Jaulmes S, Elfakir A, Quarton M, Brunet F, Chopin C (1997) Structure cristalline de la phase haute température et haute pression de $Mg_3(PO_4)_2$. J Solid State Chem 129:341–345

Leyx C, Chopin C, Brunet F, Schmid-Beurmann P, ParraT (2002) Towards a thermodynamic database for phosphate minerals: volume properties of Mg-phosphates and phase relations in the system MgO–Al_2O_3–P_2O_5–SiO_2–H_2O. IMA 18th general meeting, Edinburgh, Programme with Abstracts, p 240

Lodders K (1999) Revised thermochemical properties of phosphinidene (PH), phosphine (PH3), phosphorus nitride (PN), and magnesium phosphate ($Mg_3P_2O_8$). J Phys Chem Ref Data 28:1705–1712

Lyon JE, Fox TU, Lyons JW (1966) Phosphate bonding of magnesia refractories. Am Ceram Soc Bull 45:1078–1081

Miltenburg JC van, Genderen ACG van, Berg GJK van den (1998) Design improvements in adiabatic calorimetry. The heat capacity of cholesterol between 10 and 425 K. Thermochim Acta 319:151–162

Miltenburg JC van, Berg GJK van den, Bommel MJ van (1987) Construction of an adiabatic calorimeter. Measurement of the molar heat capacity of synthetic sapphire and of *n*-heptane. J Chem Thermodyn 19:1129–1137

Oetting FL, McDonald RA (1963) The thermodynamic properties of magnesium orthophosphate and magnesium pyrophosphate. J Phys Chem 67:2737–2743

Preston-Thomas H (1990) The International Temperature Scale of 1990 (ITS-90). Metrologia 27:3–10

Raade G (1990) Hydrothermal syntheses of Mg_2PO_4OH polymorphs. N Jb Miner Mh 1990:289–300

Raade G, Rømming C (1986) The crystal structure of ε-Mg_2PO_4OH, a synthetic high-temperature polymorph. Zeit Kristallographie 177:1–13

Sarkar AK (1990) Phosphate cement-based fast-setting binders. Am Ceram Soc Bull 69:234–238

Sata T (1997) Phase relations in the system $Ca_3(PO_4)_2$–$CaMg(SiO_3)_2$–$MgSiO_3$–SiO_2. J Ceram Soc Japan 105:26–30

Stevens CG, Turkdogan ET (1954) The heats of formation of trimanganous phosphate and trimagnesium phosphate. Trans Faraday Soc 50:370–373

Sutor D, Wooley SE, Ellingsworth JJ (1974) Some aspects of the urinary stones in Great Britain and Northern Ireland. Brit J Urol 46:275–288

Théodoret, Lenzi J, Roux P, Bonel G, Lenzi M (1987) Comportement sous haute pression d'orthophosphates mixtes de calcium et de cobalt Ca_{3-x} $Co_x(PO_4)_2$, $0{,}40 < x < 3$. Rev Chim Minér 24:478–488

Yang Q, Zhu B, Wu X (2000) Characteristics and durability tests of magnesium phosphate cement-based material for rapid repair of concrete. Materials and Structures 33:229–234